PHYSICAL REVIEW B

CONDENSED MATTER

THIRD SERIES, VOLUME 36, NUMBER 7 1 SEPTEMBER 1987

Spectral hole burning by population storage in Zeeman sublevels of $LaF_3:Nd^{3+}$

R. M. Macfarlane and J. C. Vial*

IBM Almaden Research Center, 650 Harry Road, San Jose, California 95120-6099

(Received 9 February 1987)

We demonstrate a new mechanism for optical spectral hole burning in which population is stored in electronic Zeeman sublevels. This is shown by optical pumping the ground-state Kramers doublet of the $^4I_{9/2} \leftrightarrow {}^2H_{11/2}$ (6248.9 Å) and $^4I_{9/2} \leftrightarrow {}^4G_{5/2}$ (5777.1 Å) transitions of $LaF_3:Nd^{3+}$ with a narrow-band cw dye laser. Experiments were carried out at 1.6 K in external fields of ~ 100 G. The Zeeman shift of the resulting antiholes and holes makes an assignment of these structures possible. Hole recovery times of hundreds of milliseconds are shorter than expected at these low temperatures and fields and provide evidence for optical spectral diffusion caused by mutual spin flips in the ground state.

I. INTRODUCTION

Spectral hole burning, or selective bleaching of inhomogeneously broadened absorption lines, is now known to occur by a number of different mechanisms. On one hand, there are mechanisms such as selective photochemistry involving the breaking of chemical bonds,[1] photoionization,[2] or photoinduced modifications of local structure in glasses.[3] These lead to persistent holes which, in addition to their great utility for high-resolution spectroscopy, have been proposed as the basis for frequency-domain optical storage.[4] On the other hand, there are mechanisms in which optical pumping of metastable population reservoirs occurs. Population may be stored in metastable optical levels,[5] or in hyperfine,[6] or superhyperfine levels.[7] In these cases the holes are rather short lived (ranging from milliseconds to minutes) but provide the means to carry out a new and powerful form of high-resolution laser spectroscopy in which electric, magnetic, and hyperfine interactions as well as numerous relaxation phenomena,[8] can be studied with new precision.

We report here the use of population storage in Zeeman levels of a Kramers doublet ("Zeeman storage") to observe spectral hole burning. It is known from ESR (Refs. 9–13) and optical[14] measurements that the spin-lattice relaxation time T_1^K between the two components of a Kramers doublet ψ_+ and ψ_- can be as long as several seconds. It is also known that this relaxation time is a strong function of magnetic field (H) since Zeeman mixing of different Kramers doublets is required to break the exact time-reversal symmetry between ψ_+ and ψ_- and thus allow direct phonon relaxation between them. The density of phonon states at the Zeeman splitting frequency $\Delta(H)$, in the Debye approximation, is proportional to H^2. This leads to an H^{-4} dependence of the spin-lattice relaxation time for $\Delta \ll kT$.[15]

In hole-burning spectroscopy, unlike ESR, it is possible, in fact preferable, to work at lower fields and smaller values of $\Delta(H)$, where it is expected that even longer population storage times will be available. The realization of very long spin-lattice relaxation times in Kramers-doublet systems depends, however, on the absence of relaxation mechanisms other than the one-phonon "direct" process. Sabisky and Anderson[14] and Hutchison *et al.*[10] have shown, for example, that T_1^K can be very sample dependent and much shorter than that expected from the direct process, presumably reflecting the role of other paramagnetic impurities. This emphasizes the need for careful attention to sample purity in experiments involving Zeeman storage.

Another factor which must be considered is spectral diffusion in the ground state due to electron spin-flip-flop processes which contribute to the transverse relaxation time T_2^K rather than T_1^K and will lead to decay of the optical spectral hole. This is because the frequency selectivity of the hole-burning process applies only to the initially excited ions. If spectral diffusion occurs in the ground state, the optical probing step will involve ions sitting in different crystal environments from those originally burned and inhomogeneous broadening effects will fill in the hole.[8] For this reason low doping levels are desirable.

II. THE ZEEMAN STORAGE PROCESS

Hole burning is produced by optical pumping of the ground-state Zeeman levels. In other words, a narrow-band laser transfers population from one Zeeman sublev-

el of the ground state to another via excitation to an excited state and subsequent relaxation to a different ground-state component. The characteristic signature which one would predict for the Zeeman storage mechanism, is the appearance of antiholes, or increased absorption, shifted by the Zeeman splittings from the central hole at the laser frequency. Figure 1 shows the pattern of holes and antiholes expected for an optical transition between two Kramers doublets. The intensities were calculated under the reasonable assumption that the transition strengths between the levels $g_+e_+ = g_-e_-$ and between $g_+e_- = g_-e_+$ where g and e label ground and excited states and $+$ and $-$ the Kramers-doublet components (see Fig. 1). This is certainly true at low fields. The features to note are the following.

(i) Holes occur at the laser frequency ω_L and side holes at $\omega_L \pm g_2\mu_B H$, where g_2 is the excited-state g value.

(ii) Antiholes occur, shifted from the central hole by the ground-state Zeeman splitting $g_1\mu_B H$ and by the sum and difference of ground and excited state g values.

Four sets of ions need to be considered in constructing the hole and antihole pattern—these sets having different transitions resonant with the fixed laser frequency, the shift being produced by the inhomogeneous broadening. Some modification of the intensities in these patterns clearly occurs if the Zeeman splittings are greater than the inhomogeneous linewidth of the optical

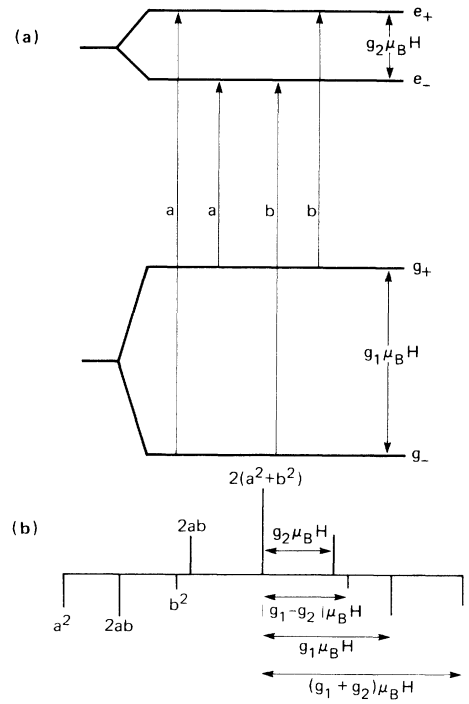

FIG. 1. (a) Optical transitions between Zeeman-split components of two Kramers doublets with intensities a and b. (b) Hole (upwards) and antihole (downwards) pattern expected for Zeeman storage hole burning following optical pumping of the sublevels of the ground Kramers doublet. The pattern is symmetrical with relative intensities shown on the left and splittings on the right.

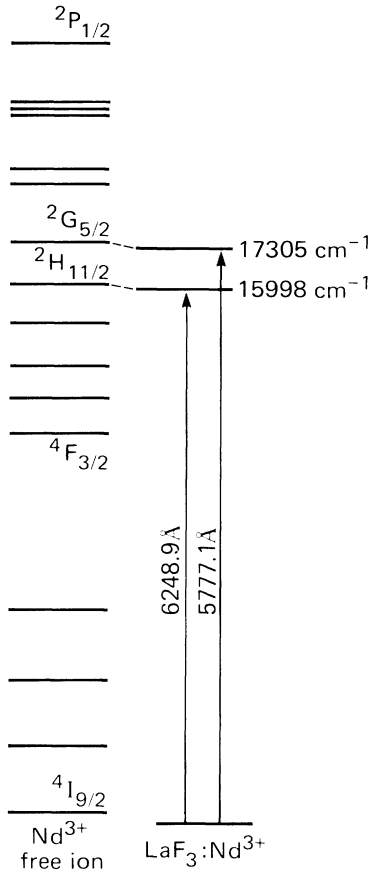

FIG. 2. Energy-level diagram for the Nd^{3+} ion. The two transitions studied in this paper are shown by the vertical arrows.

transitions or if the ground-state Zeeman splitting is larger than kT. The intensities of holes and antiholes also depend on the strength of the transitions (a,b) between the individual Zeeman components. This depends on the crystal site symmetry and on the particular optical transition involved, so that very different hole-burning patterns can be observed in practice.

Our measurements were made at 1.8 K on a sample of LaF_3:Nd^{3+} containing 0.005 at.% Nd^{3+}. The overall energy-level diagram for Nd^{3+} is shown in Fig. 2. Two transitions were studied in this work—those from the ground state to the lowest component of $^2H_{11/2}$ at 6248.9 Å and to the lowest component of $^4G_{5/2}$ at 5777.1 Å. The site symmetry of Nd^{3+} in LaF_3 is C_2 (Ref. 16) and the external magnetic field was always applied parallel to the crystal c axis, i.e., perpendicular to the three C_2 axes. In this case, no strict selection rules control the intensities a,b of Fig. 1 and the different hole-burning patterns observed for different transitions reflect the different intensity ratio a/b.

III. THE $^4I_{9/2} \leftrightarrow {}^2H_{11/2}$ TRANSITION

For this transition, at 6248.9 Å, a fluorescence excitation spectrum was measured using a cw dye laser of width ~2 MHz (see Fig. 3). The inhomogeneous linewidth is

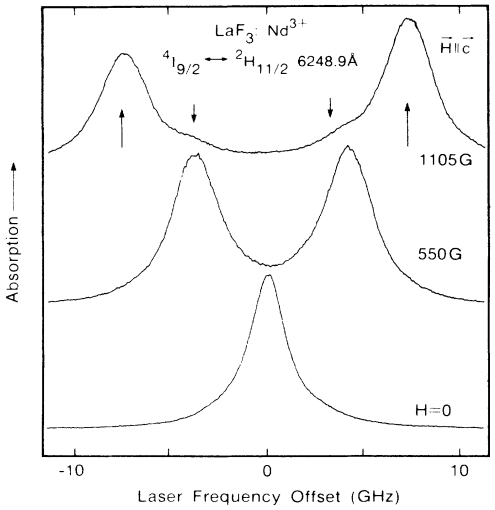

FIG. 3. Zeeman splitting of the 6248.9-Å absorption arising from the transition from the lowest component of $^4I_{9/2}$ to the lowest component of $^2H_{11/2}$. Note the large difference between the intensities of the four Zeeman components, which are marked by the vertical arrows.

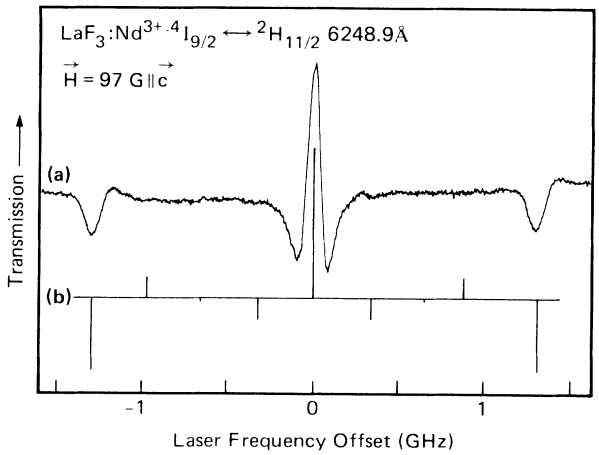

FIG. 4. Hole-burning spectrum of the 6248.9-Å transition in an external magnetic field of 97 G at 1.6 K. The splitting of 1.3 GHz demonstrates that population storage occurs in the Zeeman sublevels. The antiholes adjacent to the central hole are assigned to superhyperfine storage. The stick pattern below is that expected from the Zeeman intensities in Fig. 3.

2.4 GHz and a conventional Zeeman effect measurement for $\mathbf{H}\|\mathbf{c}$ showed that for this transition $a/b \simeq 7$ (Fig. 3). The ground-state g tensor has been measured by Schulz and Jeffries[9] and for $\mathbf{H}\|\mathbf{c}$ their results give $g_1 = 2.41$.

Hole-burning measurements were carried out using two single-frequency cw dye lasers each with a frequency jitter width of ~ 2 MHz. One laser was tuned to the center of the inhomogeneous line profile and weakly focused to produce a hole about 25% deep. Simultaneously the second laser at lower intensity was used to probe the hole in a fluorescence excitation spectrum, monitoring the emission from $^4F_{3/2}$.

A typical spectrum of holes and antiholes for $|\mathbf{H}(\|\mathbf{c})| = 97$ G is shown in Fig. 4. Also shown is the pattern of holes and antiholes expected using the intensity ratio $a/b = 7$ obtained from Fig. 2. Although this ratio was measured at high fields (1.1 kG), there will be no field dependence of this ratio at such low fields. Zeeman antiholes are seen only for the transitions corresponding to the sum of ground and excited state of g values, the intensity of the other two pairs of antiholes being too small to observe. The assignment of the antihole was made from the measurement of its frequency shift with magnetic field shown in Fig. 5. From Fig. 3 we see that the sum of the ground- and excited-state g values $g_1 + g_2 = 9.6$ and this is the value obtained also from Fig. 5. In addition to the Zeeman antiholes, a symmetrical pair of antiholes is observed close to the central hole. They are assigned to antiholes arising from optical pumping of superhyperfine levels, i.e., those due to coupling between the electronic magnetic moment of Nd^{3+} and the nuclear moment of the fluorine neighbors. Hole burning due to this mechanism has been observed in CaF_2:Pr^{3+}.[7] Pumping into this reservoir, of course, depletes intensity from the Zeeman antiholes. This may account for the fact that the antihole at $g_1\mu_B H$ and the hole at $g_2\mu_B H$ are not observed, but quantitative agreement has not been obtained.

The appearance of sharp side holes is known from numerous studies of the optical pumping of hyperfine components of electronic singlet levels.[6] In general, however, inhomogeneous broadening of the sublevel transitions can broaden the side holes. In the present case, crystal strains do not contribute to the separation between the two Kramers levels and sharp side holes are also seen. This may not always be the case for non-Kramers levels.

IV. THE $^4I_{9/2} \leftrightarrow {}^4G_{5/2}$ TRANSITION

The transition to the lowest component of $^4G_{5/2}$ occurs at 5777.1 Å and has an inhomogeneous width of ~ 3 GHz in this sample. Hole-burning measurements were

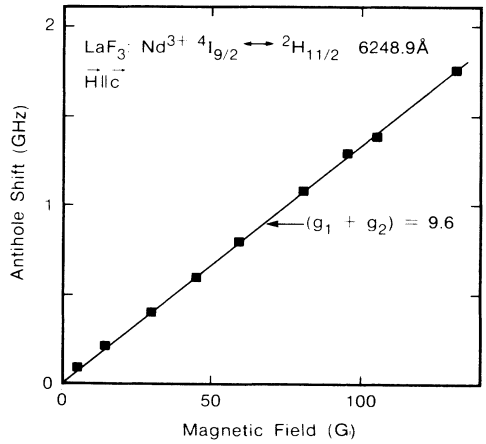

FIG. 5. Shift of the Zeeman antihole as a function of field showing that it corresponds to the sum of the ground- and excited-state g values. This is expected to be the strongest antihole (see Fig. 4).

carried out in a slightly different manner from those of Sec. III in that one laser was used for hole burning and probing. The frequency of the laser was scanned repetitively to probe the hole with a period of ~200 ms in between for hole burning. Multiple burn and probe cycles were averaged—again, using a fluorescence excitation method and monitoring emission from $^4F_{3/2}$. No attenuation was used between the burn and probe parts of the cycle. The delay between burning and probing was kept small compared to the lifetime of the sideholes which was approximately hundreds of milliseconds.

Several features of the hole-burning spectrum (Fig. 6) are different from those of the $^2H_{11/2}$ line. In the present case H_0 was still parallel to the c axis but the laser polarization was perpendicular to c.

For this geometry, conventional Zeeman measurements[17] show that the intensity of the four components of the 5777.1 Å line are approximately equal, i.e., $a/b \sim 1$. The pattern of holes and antiholes expected in this case is also shown in Fig. 6. The side hole at the excited-state Zeeman frequency is now clearly seen and the g value obtained from this, $g_2 = 1.07$, is in good agreement with the value of 1.12 obtained by Buisson *et al.*[17] using fluorescence excitation spectroscopy at high fields (26 kG). In addition, there is an antihole due to Zeeman storage, this time corresponding to the ground-state g value. In Fig. 7, the magnetic field dependence of the hole and antihole positions are plotted, yielding the ground- and excited-state g values. Although there is generally reasonable agreement with the expected intensity pattern, some discrepancies remain. Again, the spectrum is complicated by the presence of superhyperfine structure associated with the holes and antiholes, and the antihole at the difference between ground and excited Zeeman energies is close to the hole at the excited-state splitting. Another note of caution is that since the site symmetry is not axial, the σ spectrum can show some anisotropy for different orientations of E_L in the plane perpendicular to the c axis and the

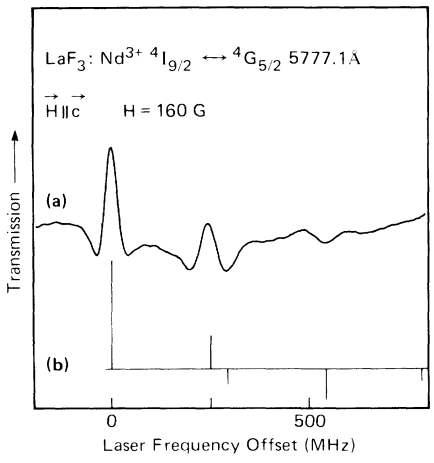

FIG. 6. Hole-burning spectrum of the 5777.1-Å $^4I_{9/2} \leftrightarrow G_{5/2}$ transition in a field of 160 G at 1.6 K. The pattern of holes and antiholes expected for $a \sim b$ (see Fig. 1) is shown below. Again, the presence of optical pumping of superhyperfine levels is shown by the antiholes adjacent to the holes.

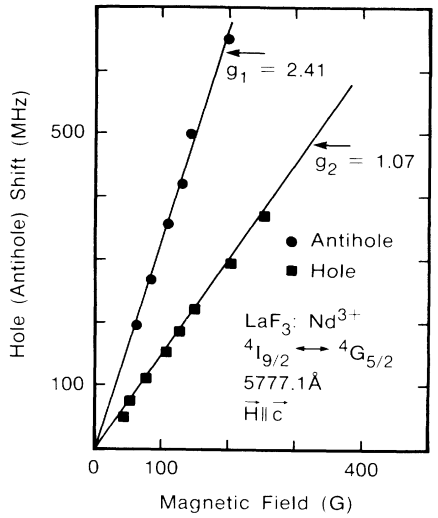

FIG. 7. Hole and antihole shifts for the pattern of Fig. 6 as a function of the external magnetic field. This shows that the main side hole shifts at a rate given by the excited-state g value and the antihole like the ground-state g value. This is expected for $a/b \sim 1$.

Zeeman pattern of Buisson *et al.*[17] may have been at a different angle than for our geometry.

V. DISCUSSION

We have shown that population storage in the Zeeman components of a Kramers doublet can be a very useful mechanism for the production of rather long-lived holes (here approximately hundreds of milliseconds). This mechanism is probably rather widespread especially at low temperatures where spin-lattice relaxation rates are long. In many cases it may be the only mechanism available for hole burning although here we find evidence for a competing process involving optical pumping of superhyperfine levels resulting from Nd-F coupling. The Zeeman coefficients of the pattern of holes and antiholes were used to assign the transitions contributing to this pattern. The hole recovery times are significantly shorter than the many seconds expected from spin-lattice relaxation of the Nd^{3+} ground levels[9] extrapolated to our measuring fields. This effect has been noted before in ESR (Ref. 9) and optical[14] measurements and has been attributed to the possible presence of low concentrations of other paramagnetic impurities. An additional contribution is expected here due to spectral diffusion involving mutual Nd^{3+} spin-flip-flops in the ground state. This leads to hole filling because the depleted population contains ions other than those which were selectively excited. In fact, the hole-burning method described here provides a new tool for studying this effect. One advantage that Zeeman storage hole burning has is the ability to measure over a wide range of magnetic fields. In addition, it provides a mechanism for detection of electron-spin coherent transients in a similar manner to that demonstrated for nuclear-spin transients.[18]

*Present address: Laboratoire de Spectrometrie Physique, Université de Grenoble, Boite Postale 87, 38402 Saint Martin d'Herès, Cedex, France.

[1]A. A. Gorokhovskii, R. K. Kaarli and L. A. Rebane, Pis'ma Zh. Eksp. Teor. Fiz. **20**, 474 (1974) [JETP Lett. **20**, 216 (1974)]; H. de Vries and D. A. Wiersma, Phys. Rev. Lett. **36**, 91 (1976).

[2]R. M. Macfarlane and R. M. Shelby, Opt. Lett. **9**, 533 (1984).

[3]B. M. Kharlamov, R. I. Personov, and L. A. Bykovskaya, Opt. Commun. **12**, 216 (1974); G. J. Small, in *Spectroscopy and Excitation Dynamics of Condensed Molecular Systems,* edited by V. M. Agranovich and R. M. Hochstrasser (North-Holland, Amsterdam, 1983).

[4]G. Castro, D. Haarer, R. M. Macfarlane, and H. P. Trommsdorff, U. S. Patent 4 101 976 (1978); W. E. Moerner, J. Molec. Electron. **1**, 55 (1985).

[5]A. Szabo, Phys. Rev. B **11**, 4512 (1975).

[6]L. E. Erickson, Phys. Rev. B **16**, 4731 (1977).

[7]R. M. Macfarlane, R. M. Shelby, and D. P. Burum, Opt. Lett. **6**, 593 (1981).

[8]R. M. Shelby, R. M. Macfarlane, and C. S. Yannoni, Phys. Rev. B **21**, 5004 (1980).

[9]M. B. Schulz and C. D. Jeffries, Phys. Rev. **149**, 270 (1966).

[10]C. A. Hutchison, Jr., M. D. Kemple, and Y.-T. Yen, Phys. Rev. Lett. **33**, 937 (1974).

[11]R. L. Orbach and H. J. Stapleton, in *Electron Paramagnetic Resonance,* edited by S. Geschwind (Plenum, New York, 1972).

[12]R. C. Mikkelson and H. J. Stapleton, Phys. Rev. **140**, A1968 (1965).

[13]B. W. Magnum and R. P. Hudson, J. Chem. Phys. **44**, 704 (1966).

[14]E. S. Sabisky and C. H. Anderson, Phys. Rev. B **1**, 2028 (1970).

[15]J. H. Van Vleck, J. Chem. Phys. **7**, 72 (1939); Phys. Rev. **57**, 426 (1940).

[16]A. Zalkin, D. H. Templeton, and T. E. Hopkins, Inorg. Chem. **5**, 1466 (1966); B. R. Reddy and L. E. Erickson, Phys. Rev. B **27**, 5217 (1983).

[17]R. Buisson, J. Q. Liu, and J.-C. Vial, J. Phys. (Paris) **45**, 1553 (1984).

[18]R. M. Shelby, C. S. Yannoni, and R. M. Macfarlane, Phys. Rev. Lett. **41**, 1739 (1978).